

Optimization of Electrochemical Phosphate Recovery from Industrial Sludge Residue Generated from Supercritical Water Oxidation Treatment with H₂O₂

M. Tekbaş*, N. Bektaş

Environmental Engineering Department, Gebze Technical University, 41400, Gebze, KOCAELİ, TURKEY

*E-mail: mtekbaz@gtu.edu.tr

Received: 7 July 2018 / Accepted: 17 August 2018 / Published: 1 October 2018

Hydrothermal oxidation in supercritical water (SCWO) is a unique and potential treatment technology for wastewater with high concentration of organics. In this process, oxidants and supercritical water dissolved organic molecules make inorganic compounds more soluble, thus creating ash-free inorganics from organic species at the bottom of SCWO reactor. This inorganic residue is very reactive and can easily dissolve into some inorganic chemical species in solvents. Electrocoagulation (EC) is a process that metal anode electrodes are dissolved into the electrolyte solution when electrical current passes through the electrodes. Electrochemical dissolution of aluminium (Al) anodes in EC reactor produces Al ions, which can be used to recover dissolved phosphate residue from acid solutions. In this study, electrochemically gained Al ions were used in the recovery of phosphate from SCWO residue. Process parameters such as reaction time, current density and pH were investigated using Box-Behnken design (BBD) as a Response Surface Methodology (RSM). Optimum operating conditions were evaluated, and the results showed accurate validities between the observed and predicted values.

Keywords: Supercritical water oxidation, sludge destruction, Box-Behnken design, mixed industrial sludge

1. INTRODUCTION

Industrial sludge, can be defined as a fluid waste that contains 0.5-10% of solid content, and is one of the major problems in industrial wastewater treatment plants [1-6]. The amount of industrial sludge is increasing by the growing use of industrial wastewater treatment technologies and the demand to meet discharge standards. Most of the wastewater treatment plant sludge (WWTPS) are dewatered using expensive techniques and subsequently discharged to landfills. However, many new regulations forbid disposal of organic waste to landfills [7,8]. Therefore, new methods for disposal of

sewage sludge must be found. Supercritical water oxidation (SCWO) with addition of oxidant can offer an effective and fast destruction method for organic and inorganic hazardous waste contents of the sludge or wastewater in a very short time [9-11]. In SCWO, organic carbon; organic and inorganic nitrogen; halogenated organic and inorganic species; sulphated organic and inorganics are transformed into carbon dioxide, nitrogen gas (N_2), their corresponding acids and sulphuric acid (Fig. 1). In the literature, several studies have shown that SWCO can effectively treat various type of organic waste [12-18]. Metals in the untreated sludge can be oxidised to their highest valency, in which they make various complexes in SCWO residues. Phosphorous present in industrial wastewater may directly pass into the generated sludge if non-effective phosphorus removal technologies are used during wastewater treatment. Phosphate is essential for all living elements, agricultural and industrial developments, and is obtained from limited natural or chemical resources. Also, discharging phosphate in wastewaters to the receiving media can cause serious environmental problems such as eutrophication. Therefore, recovery of phosphate from wastes has become an issue of concern. The recovery of phosphorous does not only help in avoiding nutrient enrichment of receiving streams but is also a good alternative for use as either a fertilizer or a raw material by the related industries [19-21].

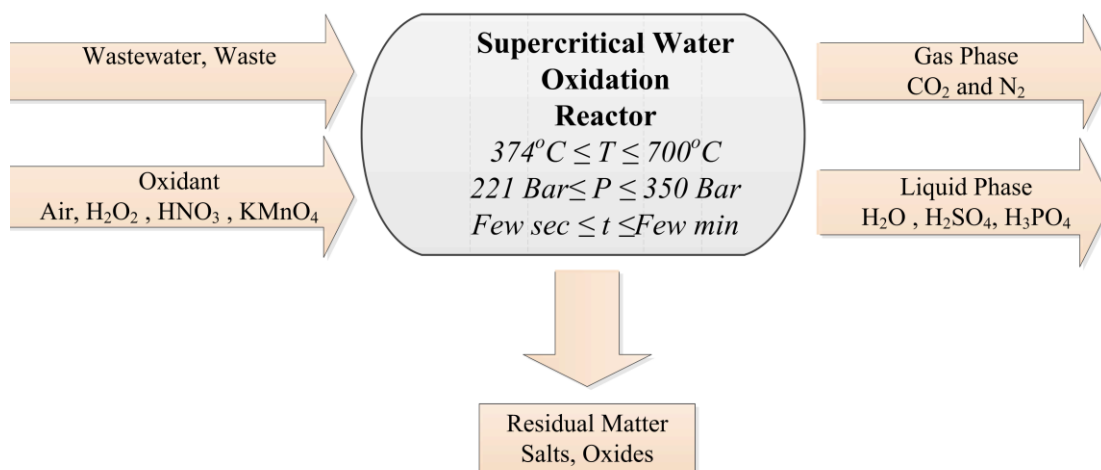


Figure 1. Schematic presentation of SCWO process.

Electrocoagulation (EC) process provides a simple, comparatively shorter treatment time and is economical for the treatment of wastewater without adding any chemicals [22-26]. In EC, metal electrodes are dipped in the electrolyte solution and dissolution of the anode occurs when electrical current passes through the electrodes, generating hydroxide ions (OH^-) and H_2 gas by reactions at anode and cathode, respectively. The multiple electrochemical reactions that simultaneously occur at the anodes and cathodes are given by Eq 1-4 (Fig. 2-a). Dissolved Al^{3+} ions from anodes can react with dissolved PO_4^{3-} ions in SCWO residue as well as OH^- to form solid $AlPO_4$ and $Al(OH)_3$ according to complex precipitation kinetics (Eq 5-6). Other metal ions dissolved in the residue may react with phosphate ions (Eq. 7). As shown in Eq. (6) superfluous Al^{3+} could be co-precipitated as $Al(OH)_3$, with the concurrent formation of $AlPO_4$ thus, electrochemically generated precipitate is a mixture of $AlPO_4$, $Al(OH)_3$ and $M_x(OH)_y$ if other metal ions are present. Formation of these chemicals depend

on many factors including pH range [22-30]. Therefore, an inorganic residue from the SCWO enables phosphates recovery from the sewage sludge due to precipitation reactions (Fig. 2-b).

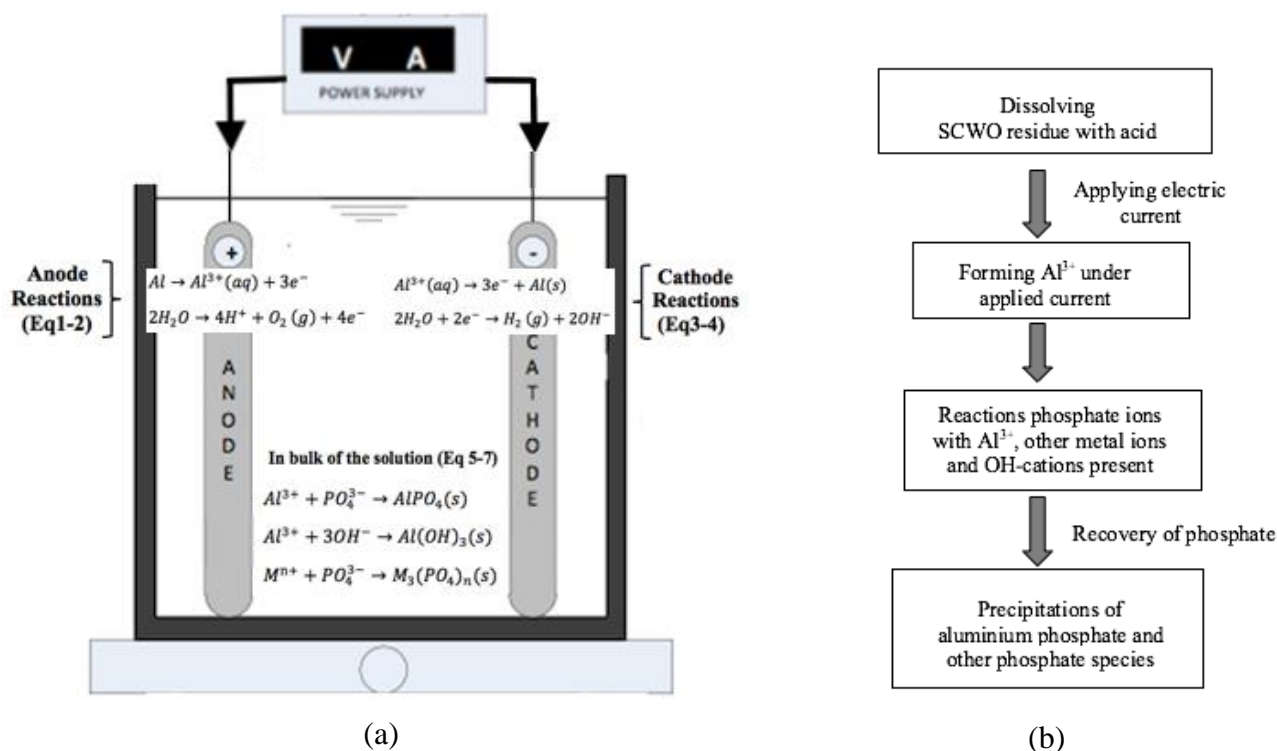


Figure 2. a) Main reactions (Eq 1-7) may occur in EC reactor with Al electrodes for SCWO residue leach solution (M represents metal ions that may be present in the residue)
b) The mechanism of phosphate recovery by electrocoagulation

Phosphate removal by EC have been studied by many researchers. These papers mostly investigated various EC process parameters effecting removal rate, such as current density, time, initial concentration, temperature, pH of the solution, salt concentrations and electrolyte type [31-34]. Phosphate recovery from different environmental samples by EC were also explored in recent research papers. Phosphate removal and recovery from dairy manure using EC process with four different electrode materials was evaluated by Zhang et al, 2016. Their results showed EC with low carbon steel electrode achieved the highest P recovery (96.7%). In another study, phosphorous recover as struvite from synthetic wastewater using magnesium-air fuel cell EC was investigated [35]. The result showed that the rate determining step behind struvite recovery process was Mg electrode dissolution rate, which increased with current density. Other effective parameters were found as Mg:P dosage ratio and pH. Furthermore, they reported that electrochemically formed Mg and P can be precipitated as struvite, which is a slow-releasing fertilizer for the recovery of phosphorous from wastewater. Huang et al 2017 [36] studied the feasibility of phosphate recovery from anaerobic sludge supernatant using EC. Their study focused on comparison between EC and chemical precipitation and the effect of EC process parameters such as solution pH, reaction time, alkalinity and reagent dosage on the recovery of phosphate were studied.

The literature studies focusing on phosphorous removal from SCWO residue are very limited in literature. In the present study, phosphate in SCWO residue was extracted in acidic environment then recovered by precipitation using electrochemically *in situ* generated aluminium ions in an electrochemical cell. Factorial experiments are generally used in this area of research to obtain more precise results, due to the multiple factors influencing the process. The reaction parameters such as time, pH, current density and energy consumption were investigated using Box-Behnken design (BBD) as a Response Surface Methodology (RSM), to evaluate the optimum operating conditions for the recovery of PO_4^{3-} ions. The novelty of this study is based on electrochemical recovery of phosphate from SCWO residue of mixed industry sludge containing inorganic salts and hazardous substances. Also, the demand for new phosphate resources and recovery of phosphate has become an interesting area of research, since phosphate is a vital substance in many industrial and agricultural activities.

2. MATERIAL AND METHODS

2.1. Chemicals and Analytical Methods

Sludge samples were collected from mixed industrial wastewater treatment plant and treated using SCWO with H_2O_2 as an oxidant source. The main characterisation of the sludge sample and results of the SCWO treatment of sludge are given in another scientific study [37]. Total solids and phosphate content of raw mixed sludge sample were determined as 6.5% and 208 mg/L, respectively.

The semi-quantitative energy dispersive spectrometric (EDS) analyses were conducted using a Scanning Electron Microscope (SEM) with EDS module, (Philips XL 30 SFEG) to identify PO_4^{3-} ions on three different selected surface areas (SSA) of SCWO residue and EC participate samples. FTIR analyses of EC participates were conducted with Perkin Elmer Spectrum-100 to investigate surface structure and aid identification of surface reaction species. Energy consumptions of the EC process at each experimental condition were calculated using the following equation [38-40];

$$E = \frac{IUt}{V} \quad (8)$$

Where; E is used energy (kWh/m³), I is current intensity (A), U is voltage (V), t is time (h), V is treated solution volume (m³)

2.2. Experimental Set-up and Procedure

Schematic representation of SCWO and EC reactors (65x65x105 mm) used for the electrochemical recovery of PO_4^{3-} ions are schematically given in the Fig. 3a and b, respectively. Total P recovery route was designed in two steps: The first step involved SCWO process (Oxidant rate 2, 520°C, 250 bar) and the resulting solid residue was dissolved in 0.1M HCl solution according to literature studies [41,42]. The mixture of 25 mL, 0.1 M HCl solution and 0.5 g of SCWO residue were agitated at 300 rpm for 60 min at room temperature and then total phosphate concentration was

determined by colorimetric method (Standard Methods 4500P) [43]. In the colorimetric method, samples were first, oxidized with strong acids to convert the available phosphates to orthophosphate prior to analysis. Average initial total phosphate concentration was measured as 41 ± 1 mg/L. In the second step involving EC process, acid dissolved SCWO residue was placed in the EC reactor and total phosphate ions were recovered by precipitation with electrochemically generated Al^{+3} or OH^- ions. Initial pH was adjusted according to experimental conditions using diluted NaOH. Recovery of PO_4^{3-} was calculated from total P concentrations of samples taken from the EC reactor at different time intervals.

EC reactor (250 cm^3 of active volume) used in the experimental study consists of a pair of rectangular shape electrodes made of Al (total active area of 36 cm^2). Aluminium electrodes were cleaned with acidic solution and dried after each experiment. The distance between each electrode was 30 mm. The leach solution of SCWO residue was placed in this EC reactor and electrodes were connected to a digital DC power supply (0–5 A and 0–30 V, NETES 3306D) in monopolar-parallel mode as shown in Fig. 3-b.

The EC process parameters were varied as follows: initial current intensity (10 – 36 and 25–62.5 A/m²), pH (3 – 4 and 5-6) and reaction time (10 - 65-120 min.). After each trail, the collected liquid samples were centrifuged at 5000 rpm for 3 minutes to separate flocs and subsequently filtered. The filtration residue was dried at 105°C for 1 hour and analysed for.

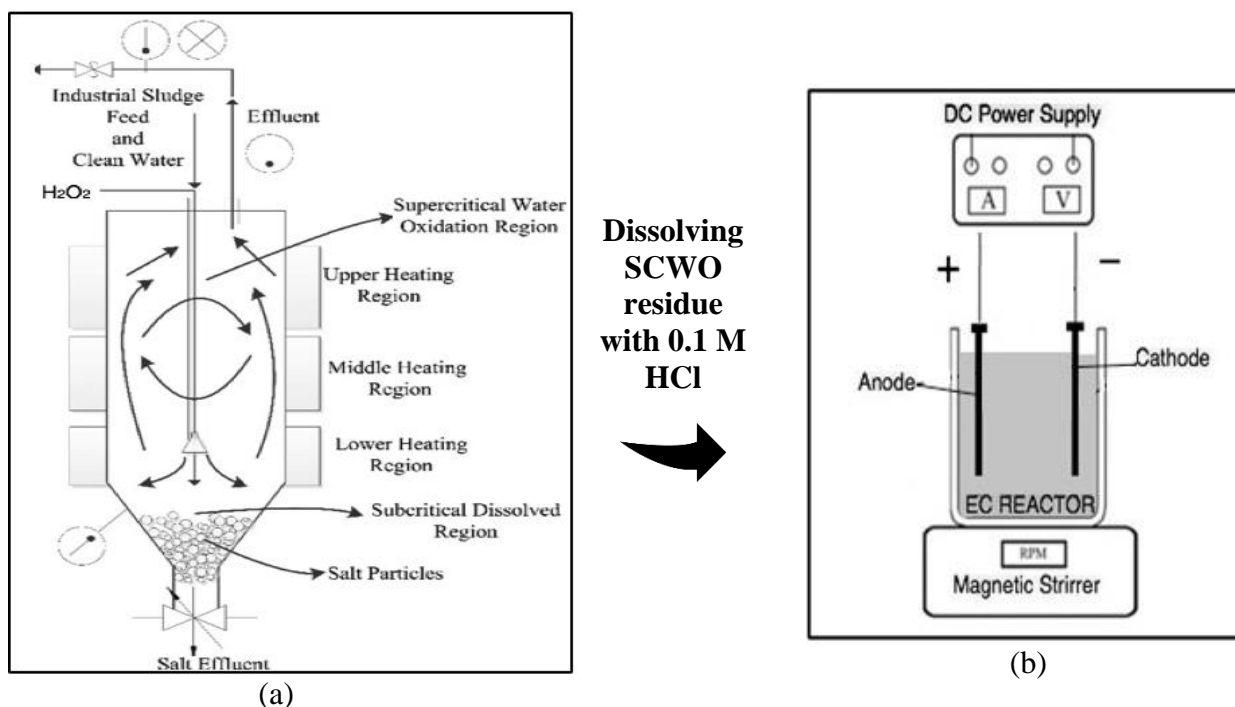


Figure 3. Schematic diagram of pilot reactor for SCWO with H_2O_2 and collection of SCWO residue (P:250 bar; T: 520°C , t:180 sec. n: 2) (a); EC experimental set-up (b) (C:208 mg/L, Al electrode).

2.3. Experimental Design

To obtain a detailed understanding of the process, experiments with numerous input independent variables require to be conducted. This can be a tedious process and often time wasting. Therefore, the used Response Surface Methodology (RSM) is applied to define the complex experiment conditions[44-46].

In this study, the Box-Behnken Design (BBD) method based on the effects of the independent variables on the responses and interactions between different variables, was applied to further evaluate the experimental data. This method requires 3 levels of each factor, that are usually located in each block within all combinations and the other factors are kept at the central [44-46]. These values can be solved using the following the second-order polynomial model equation used for each response (y):

$$y_i = \beta_0 + \sum_1^3 \beta_i X_i + \sum_1^3 \beta_{ii} X_{ii}^2 + \sum_1^3 \beta_{ij} X_{ij} \quad (\text{Eq.8})$$

where, β_0 , β_i , β_{ii} and β_{ij} are the regression coefficients for intercept, linear, quadratic and interaction terms, respectively;

x_i , and x_{ij} are the independent variables.

In this study, initial pH (x_1), current density (x_2) and reaction time (x_3) were used as three blocks for the 3 BBD factors. The fixed responses in this process are recovery of phosphate (y_1) and energy consumption (y_2). The levels of original and coded factors for operating parameters are given in Table 2. Each response was solved from a second-order polynomial model using MINITAB software (version 18). The coefficient of determination (R^2) exhibited polynomial model characteristics. The statistical significance of the model was also controlled by Fisher F-test and results evaluated by P-value and F-value.

Table 2. Range of operating parameters for original and coded factors

Variables	Code	Real values of coded level		
		-1	0	+1
pH	x_1	3	4.5	6
Current Density (A/m^2)	x_2	10	36.25	62.5
Reaction Time (t/min)	x_3	10	65	120

3. RESULTS AND DISCUSSION

3.1. Analysis of Box-Behnken Design Experiments

Process parameters were optimized by Box-Behnken design experiments model with some operational parameters (initial pH, current density and reaction time) for recovery of PO_4^{3-} and energy consumption. Table 3 presents the Box-Behnken design for initial pH (x_1), current density (x_2) and reaction time (x_3) for fifteen experimental trials. A full second-order polynomial (quadratic) model in Equation 8 was used to calculate phosphate recovery (y_1) and energy consumption (y_2). The BBD suggested second order polynomial model for coded factors of y_1 (PO_4^{3-} recovery rate, %), y_2 (Energy consumption, kwh/m^3) and their respective operating variables are given below (Eq. 9-10):

$$Y_1 = -14.5 + 9.39 X_1 + 0.895 X_2 + 1.587 X_3 - 0.00417 X_3 X_3 - 0.1 X_1 X_3 - 0.00848 X_2 X_3 \quad (\text{Eq. 9})$$

$$Y_2 = 8.62 - 0.95 X_1 - 0.081X_2 - 0.238X_3 + 0.00953 X_3 X_3 + 0.0039 X_1 X_3 + 0.00681 X_2 X_3 \quad (\text{Eq. 10})$$

A plot of PO_4^{3-} recovery (%) and energy consumption E (kWh/m^3) obtained from the second-order regression model versus the observed value showed a straight line (plots are not given here). The regression coefficients (R^2) for recovery of PO_4^{3-} (%) and energy consumption E (kWh/m^3) removals were calculated as 0.911 and 0.931, respectively, this shows accurate validity between dependent variables and the independent variables of the quadratic model.

Table 3. Box-Behnken design with three experimental factors for the measured and model predicted values of total P recovery (%) and energy consumption E (kWh/m^3)

Run	pH (x_1)	Current Density J (A/m^2) (x_2)	Reaction Time t (min) (x_3)	y_1, PO_4^{3-} Recovery Rate (%)		$y_2, \text{Energy Consumption kWh/m}^3$	
				Experimental	Predicted	Experimental	Predicted
1	3	36.25	10	45.41	55.47	2.197	0.542
2	6	36.25	120	99.72	95.73	15.14	14.94
3	4.5	10	10	49.33	49.28	1.656	4.395
4	4.5	36.25	65	99.32	99.32	3.958	4.530
5	4.5	36.25	65	99.36	99.32	3.534	4.530
6	4.5	36.25	65	99.21	99.32	3.675	4.530
7	6	36.25	10	78.53	80.63	1.174	-1.547
8	3	62.50	65	99.86	101.52	22.42	19.64
9	4.5	62.50	120	99.97	93.95	41.40	39.87
10	4.5	10	120	99.33	105.37	1.656	1.232
11	3	10	65	88.12	88.46	0.781	0.647
12	6	10	65	89.56	97.12	0.741	-1.441
13	4.5	62.50	10	98.94	86.827	2.101	3.735
14	3	36.25	120	99.61	103.58	14.88	17.03
15	6	62.50	65	99.82	110.18	14.87	17.55

The ANOVA was used to show the significance and adequacy of the model. The ANOVA of regression parameters for the predicted response surface quadratic model, EC phosphate recovery rate and energy consumption are given in Table 4.

Table 4. ANOVA results of the predicted response surface quadratic model

Process	Model	R^2	Adjusted R^2	Adjusted Sum of Squares	Adjusted Mean Square	F-Value	P-Value
Electrocoagulation Recovery Process	PO_4^{3-} Recovery Rate	0.911	0.844	4265.03	710.84	13.64	0.001
	Energy Consumption	0.931	0.878	1691.15	281.858	17.84	<0.001

F values of regressions, defined as the ratio of mean square of the regression were found to be high enough for both calculations as shown in Table 4. Similarly, P-values were determined to be less

than 0.0001 for the second-order polynomial fitting demonstrating that the model is statistically significant.

Furthermore, the P value was investigated to assess the model validity. Values of P less than 0.05 imply that the model terms are significant, while the values higher than 0.1 show that the model terms are insignificant. Phosphate recovery rate and energy consumption by EC showed F-values of 13.84 and 17.84, respectively, according to ANOVA analysis given in Table 5-6.

Table 5. ANOVA results for response surface quadratic model of phosphate recovery by EC

Source	DF	Adjusted SS	Adjusted MS	F-Value	P-Value	Remark
Model	6	4265.03	710.84	13.64	0.001	Highly Significant
Linear	3	2799.92	933.31	17.90	0.001	Highly Significant
x1 (pH)	1	149.81	149.81	2.87	0.128	Not Significant
x2 (J)	1	652.43	652.43	12.52	0.008	Significant
x3 (t)	1	1997.69	1997.69	38.32	<0.001	Highly Significant
Square	1	593.32	593.32	11.38	0.010	Significant
x3 (t)*x3 (t)	1	593.32	593.32	11.38	0.010	Significant
2-Way Interaction	2	871.79	435.89	8.36	0.011	Significant
x1 (pH)*x3 (t)	1	272.43	272.43	5.23	0.052	Not Significant
x2 (J)*x3 (t)	1	599.36	599.36	11.50	0.009	Significant
Error	8	417.02	52.13			
Lack-of-Fit	6	417.01	69.50	11365.40	<0.001	Highly Significant
Pure Error	2	0.01	0.01			
Total	14	4682.05				

Table 6. ANOVA results for the response surface quadratic model for energy consumption by EC

Source	DF	Adjusted SS	Adjusted MS	F-Value	P-Value	Remark
Model	6	1691.15	281.858	17.84	<0.001	Highly Significant
Linear	3	1273.56	424.519	26.87	<0.001	Highly Significant
x1 (pH)	1	8.73	8.729	0.55	0.479	Not Significant
x2 (J)	1	721.25	721.254	45.66	<0.001	Highly Significant
x3 (t)	1	543.57	543.572	34.41	<0.001	Highly Significant
Square	1	31.06	31.058	1.97	0.198	Not Significant
x3 (t)*x3 (t)	1	31.06	31.058	1.97	0.198	Not Significant
2-Way Interaction	2	386.53	193.267	12.24	0.004	Significant
x1 (pH)*x3 (t)	1	0.41	0.412	0.03	0.876	Not Significant
x2 (J)*x3 (t)	1	386.12	386.123	24.44	0.001	Highly Significant
Error	8	126.37	15.796			
Lack-of-Fit	6	126.28	21.046	451.28	0.002	Highly Significant
Pure Error	2	0.09	0.047			
Total	14	1817.52				

Matching P-values were determined to be 0.001 and <0.001, respectively, implying that the model is statistically significant. Also, significances of interaction effects for process parameters investigated by ANOVA analysis are given in Table 5-6 for phosphate recovery and energy consumption, respectively.

3.2 Experimental Results

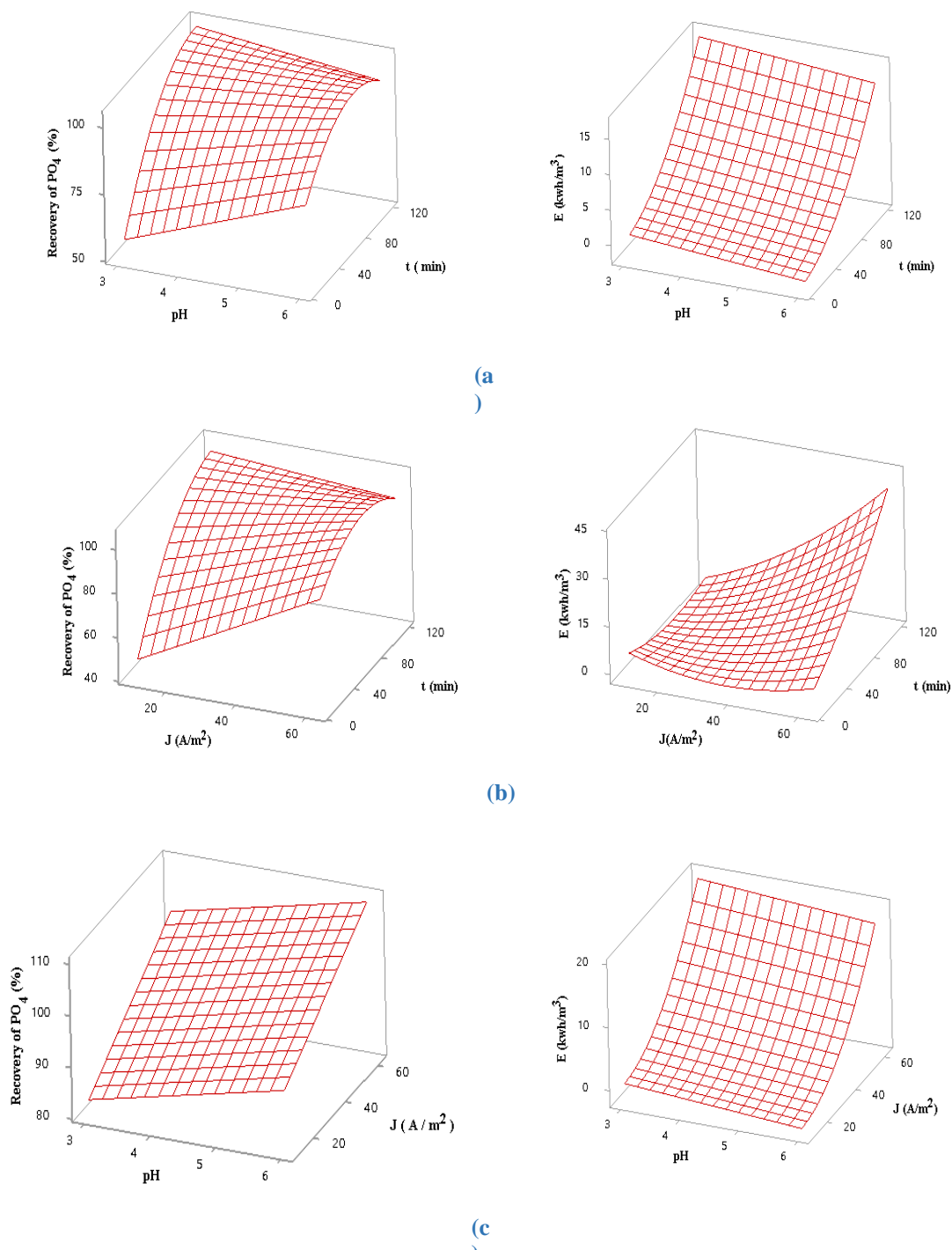


Figure 4. 3D surface plots for the recovery of PO_4 (%) and energy consumption (kWh/m³) for EC process with Al electrodes ($C= 208$ mg/L) (a) Effect of initial pH and reaction time ($J: 10$

A/m^2) (b) Effect of current density and reaction time (pH: 3) (c) Effect of initial pH and current density (t: 65 min)

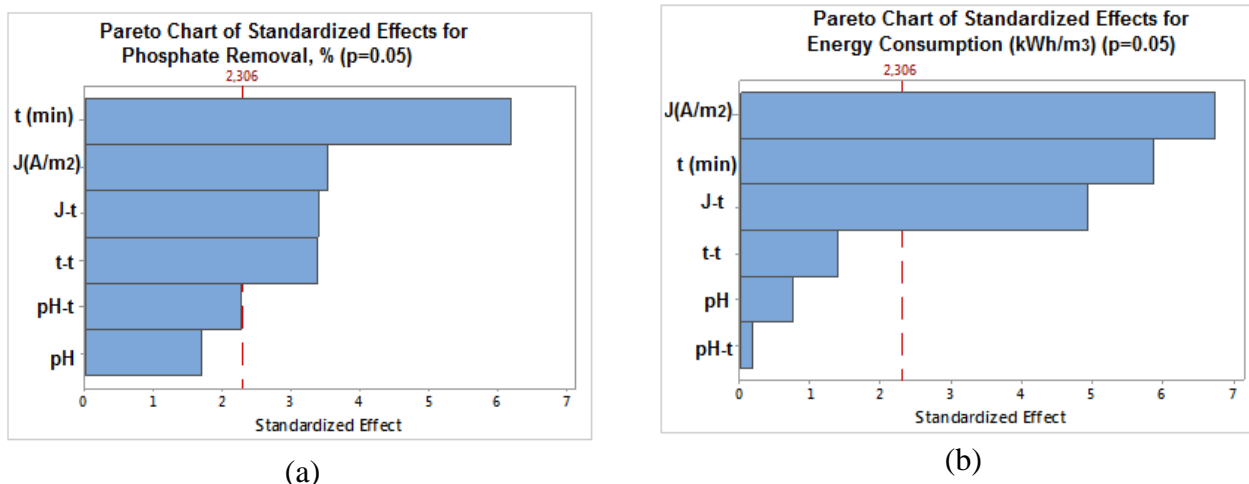


Figure 5. Pareto charts showing the effects of model factors for phosphate recovery and energy consumption.

The response surface contour plots are given in Fig.4. These graphical representations originated from the models of Eqs. (9) and (10). As can be seen from the Fig. 4, phosphate recovery increased with increase in reaction time. The pH was positively affected at initial reaction times, but low pH value and longer reaction time resulted into higher PO_4^{3-} recovery rate. This is ascribed to formation of more aluminium phosphate than aluminium hydroxide since Al^{3+} ions occur at lower pH [47-48] that freely react with PO_4^{3-} ions (Fig. 4a). All current values (at pH 3) showed low recovery rate at shorter reaction time, while higher reaction time increased recovery rates for all current densities used. This is ascribed to the formation of OH^- ions, that co-precipitated as $Al(OH)_3$, as pH value increases towards 6 [47-49]. It may also be due to formation metal hydroxides which adsorb phosphate ions and helps in coagulation of PO_4^{3-} ions as flocs. These reactions increase the recovery rate of phosphate ions. (Fig. 4 b). PO_4^{3-} recovery was also increased for all pH values at 65 minutes of EC reaction time. In general, recovery of PO_4^{3-} increased with pH and a similar trend was observed with current density (Fig. 4b-c). Energy consumption was also increased with increased current density and reaction time, this is not surprising because operation time and current density are directly proportional to energy consumption (Fig. 4 a,b,c). The cost of energy consumption for EC process was calculated in the range of 0.741-41.4 (kWh/m³) depending on current density and reaction time.

Pareto analysis on standardized main coefficients of different factors (t, J, pH) and their two-factor interactive effects on phosphate recovery and energy consumption of EC reactor are given in Fig. 5. These results showed that the most important factors for phosphate recovery and energy consumption are reaction time and current density, respectively. Pareto analysis also concludes that the relationship between the current density and time is as important as factor J in the system. It has been shown that the recovery rate is increased by longer time at lower current density, whereas higher current density can result into high recovery rate immediately at initial stages reaction. At high current

density and time, it is seen that the Al concentration in the recovery product is dominant. Available literature studies also showed that current density and time increased phosphate recovery rate [35-36].

The highest recovery rate of phosphate and energy consumption suggested by the surface response plots at the optimum experimental conditions are given in Table 5. As can be seen from these results, the experimental results, closely agree with predicted values of BBD optimisation. This result showed that the RSM is a simple method to optimize the complex process parameters using the statistical design of experiments.

Table 5. Comparison between results obtained from optimum condition experiments and the Box-Behnken design optimization

Conditions	One factor at a time experiment	Box- Behnken design optimization
pH	4.5	3.11
Current (A/m ²)	10	10
Reaction Time	120	97.14
Recovery of PO_4^{3-} (%)	99.33	99.17
Energy Consumption (E=kwh/m ³)	1.65	0.741

3.3. SEM-EDS and FTIR Analysis of Residues

Semi- quantitative SEM/EDS analyses was conducted on three different selected surface areas (SSA) of solid samples. PO_4^{3-} ions were determined as % 5.05 ± 0.331 and 5.02 ± 0.012 , for SCWO residue and EC participate respectively. These results revealed that total the P content of in SCWO residue was almost completely recovered by EC (up to %99). Further, FTIR analysis were conducted for bulk sample from EC precipitation to investigate the framework structure. In FTIR curves given in Fig. 5, the most prominent feature is the strong band in the 1000-1200 cm^{-1} region which corresponds to the P-O stretch of the structural PO_4^{3-} groups. The wide-ranging and smooth absorption bands of 400-800 and 2700-3700 cm^{-1} were related to the Al-O and O-H stretching vibration, respectively [49,50]. O-H, Al-O peaks were decreased confirming that Al ions precipitate with OH- ions (as $Al(OH)_3$) with longer reaction times (65-120 min) and moderate current densities (10-36.25 A/m²). As can be seen from Fig. 5a, AL-O peaks is very deep showing Al ions were excessively dissolved with longer reaction times and higher current density. At the same time, the band observed P-O stretch peaks at 1000-1200 cm^{-1} regions corresponds to the of the structural PO_4^{3-} groups showing that $AlPO_4$ appeared at those conditions (Fig. 6).

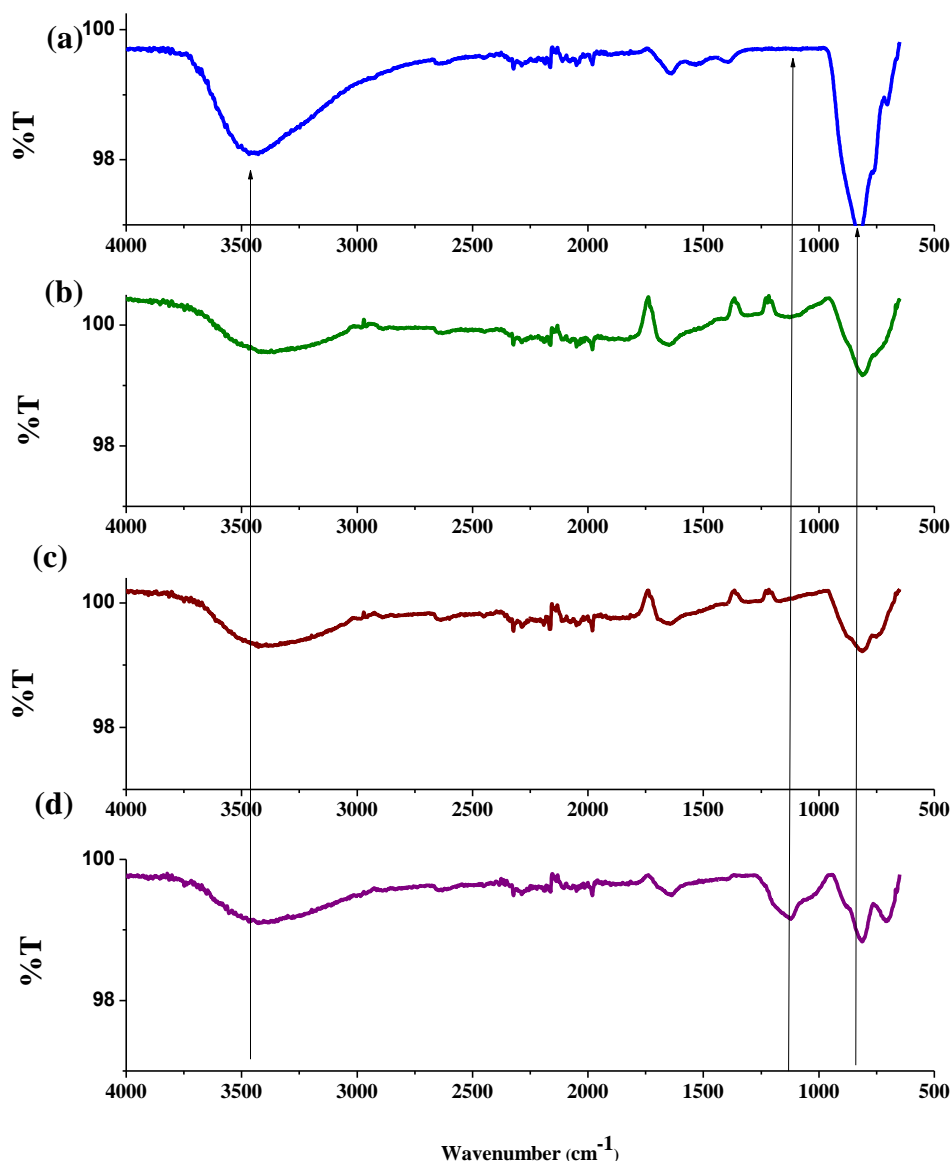


Figure 6. FTIR spectrums of four different EC process residues. (a) pH 3, 65 min., 62.5 A/m²; (b) pH 4, 10 min., 62.5 A/m²; (c) pH 6, 120 min., 36.25 A/m²; (d) pH 3, 65 min., 10 A/m².

4. CONCLUSIONS

In this study, inorganic residue was used to electrochemically recovery phosphate ions from supercritical water oxidation (SCWO) residue of mixed industrial sludge. A batch EC reactor was used to gain electrochemically dissolved Al ions for formation of mainly aluminium phosphate and other Al compounds. The effects of operating conditions such as time, pH, current density and energy consumption were investigated using Box-Behnken design (BBD) as a Response Surface Methodology (RSM). In addition, optimum operating conditions for the recovery of PO_4^{3-} ions were evaluated. Over %99 recovery rate were obtained at optimum experimental conditions with 1.65 kwh/m³ energy consumption. Box-Behnken design (BBD) results exposed that there are precise validities between the

observed and predicted values. Therefore, based on this batch scale study results, EC could be used as an innovative recovery strategy for industrial wastewater treatment sludge.

ACKNOWLEDGEMENTS

This work was funded and supported by T.C. Small and Medium Business Development and Support Administration (KOSGEB) research fund 910228.

References

1. B. Cui, F. Cui, G. Jing, S. Xu, W. Huo, S. Liu, *J. Hazard. Mater.*, 165 (2009) 511–517.
2. B.R. Gurjar, *Sludge Treatment and Disposal*, CRC Press (2001) 1-266.
3. Q. Zhang, J. Hu, D.-J. Lee, Y. Chang, Y.-J. Lee, Sludge treatment: Current research trends, *Bioresour. Technol.*, 243 (2017) 1159-1172
4. F. D. Sanin, W.W. Clarkson, P. A. Vesilind, *Sludge Engineering: The Treatment and Disposal of Wastewater Sludges*, DEStech Publications (2011) 1-25.
5. I.S. Turovskiy, P.K. Mathai, *Wastewater Sludge Processing*, John Wiley & Sons (2006) 1-60.
6. A. Raheem, V.S. Sikarwar, J. He, W. Dastyar, D.D. Dionysiou, W. Wang, M. Zhao, *Chem. Eng. J.*, 337(2018) 616-641.
7. *EU Council Directive on Urban Waste-Water Treatment*, 91/271/EC, (1991).
8. A. Kelessidis, A.S. Stasinakis, *Waste Manag.*, 32 (2012) 1186-1195.
9. J. Zhang, S. Wang, Y. Li, J. Lu, S. Chen, X. Luo, *Environ Technol.*, 38 (2017) 1949-1960.
10. S. Zhang, Z. Zhang, R. Zhao, J. Gu, J. Liu, B. Örmeci, J. Zhang, *Chem. Eng. Commun.*, 204 (2017) 265-282.
11. L. Qian, S. Wang, D. Xu, Y. Guo, X. Tang, L. Wang, *Water Res.*, 89 (2016) 118-131.
12. G. Lin, D. Xu, Z. Ma, S. Wang, Y. Guo, *Energy Procedia.*, 107(2017) 357-362.
13. L. Qian, S. Wang, D. Xu, Y. Guo, X. Tang, L. Wang, *Bioresour. Technol.*, 176 (2015) 218-224.
14. O.Ö. Söğüt, M. Akgün, *J. Supercrit. Fluids*, 43 (2007) 106-111.
15. A. Miller, R. Espanani, A. Junker, D. Hendry, N. Wilkinson, D. Bollinger, J.M. Abelleira-Pereira, M.A. Deshusses, E. Inniss, W. Jacoby, *Chemosphere*, 141 (2015) 189-196.
16. T. Hübner, M. Roth, F. Vogel, *Ind. Eng. Chem. Res.*, 55 (2016) 11910-11922.
17. D. Zou, Y. Chi, C. Fu, J. Dong, F. Wang, M. Ni, *J. Hazard. Mater.*, 248–249 (2013) 177-184.
18. B. Veriansyah, J. Kim, J. Lee, *J. Hazard. Mater.*, 147(2007) 8-14.
19. Y. Ye, H.H. Ngo, W. Guo, Y. Liu, J. Li, Y. Liu, X. Zhang, H. Jia, *Science of the Total Environment.*, 576 (2017) 159–171.
20. E.D. Roy, *Ecological Engineering.*, 98(2017)213-227
21. B. Tansel, G. Lunn, O. Monje, *Chemosphere*, 194 (2018) 504-514
22. M.Y.A. Mollah, R. Schennach, J.P. Parga, D.L. Cocke, *J. Hazard. Mater.*, 84(1) (2001) 29-41
23. K. Scott, *Electrochemical processes of clean technology*, The Royal Society of Chemistry, Cambridge, UK (1995) 1-307.
24. G. Chen, *Sep. Purif. Technol.*, 38(1) (2004) 11-41.
25. M.Y.A Mollah, P. Morkovsky, J.A.G. Gomes, M. Kesmez, J. Pargad, D.L. Cocke, *J. Hazard. Mater.*, 114(1-3) (2004) 199-210.
26. M.M. Emamjomeh, M. Sivakumar, *J. Environ. Manage.*, 90(5) (2009) 1663-1679.
27. V. Kuokkanen, T. Kuokkanen, J. Rämö, U. Lassi, *Green Sustainable Chem.*, 3(2) (2013) 89-21.
28. K. Rajeshwar, J.G. Ibanez, *Environmental Electrochemistry: Fundamentals and Applications in Pollution Sensors and Abatement*, 1st Ed.; Academic Press., San Diego (1997) 1-776.
29. Y. Ait Ouaisa, M. Chabani, A. Amrane, A. Bensmaili, Rouiba, *Procedia Eng.*, 33(2012) 98-101.
30. A.A. Bukhari, *Bioresour. Technol.*, 99 (2008) 914-921.

31. D. Franco, J. Leea, S. Arbelaeza, N. Cohenb, J.Y. Kim, *Ecological Engineering*, 108(B) (2017) 589-596
32. A. Shalaby, E. Nassef, A. Mubark, M. Hussein, *American Journal of Environmental Engineering and Science*, 2014; 1(5): 90-98
33. P.I. Omwene, M. Koby, *Process Safety and Environmental Protection*, 116 (2018) 34 – 51
34. A. Attour, M. Touati, M. Tlili, M. Ben Amor, F. Lapique, J.-P. Leclerc, *Separation and Purification Technology*, 123 (2014) 124–129
35. J. H. Kim, B. M. An, D. H. Lim, J. Y. Park, *Water Research*, 132 (2018) 200-210
36. H. Huang, D. Zhang, Z. Zhao, P. Zhang, F. Gao, *Journal of Cleaner Production*, 141 (2017) 429-438
37. M. Tekbaş, unpublished PhD Thesis Experiments, Gebze Technical University Kocaeli/TURKEY, (2018).
38. C. An, G. Huang, Y. Yao, and S. Zhao, *Sci Total Environ.*, 579 (2017) 537-556.
39. J.N. Hakizimana, B. Gourich, M. Chafi, Y. Stiriba, C. Vial, P. Drogui and J. Naja, *Desalination*, 404 (2017) 1-21.
40. D.T. Moussa, M.H. El-Naas, M. Nasser and M.J. Al-Marri, *J Environ Manage*, 186 (1) (2017) 24-41.
41. K. Stendahl, S. Jäferström, *Water Sci. Technol.*, 48 (2003) 185-190.
42. K. Stark, E. Plaza, B. Hultman, *Chemosphere*, 62 (2006) 827-832.
43. E.W. Rice, R.B. Baird, A.D. Eaton, L.S. Clesceri (Eds.); APHA, AWWA, WEF, *Standard Methods for The Examination of Water and Wastewater*; 22nd Ed.; Washington DC, USA (2012) 4108-4117.
44. K.M. Sharif, M.M. Rahman, J. Azmir, A. Mohamed, M.H.A. Jahurul, F. Sahena, I.S.M. Zaidul, *J. Food Eng.*, 124 (2014) 105-116.
45. S. Karimifard, M.R.A. Moghaddam, *Sci. Total Environ.*, 640 (2018) 772-797.
46. P.G. Mathews, M. Malnar, P.G. Mathews, *Anal. Methods Des. Pract.* (2017) 309-391.
47. I. Linares-Hernández, C. Barrera-Díaz, G. Roa-Morales, B. Bilyeu, *Chem. Eng. J.*, 148(1) (2009) 97-105.
48. J. Duan, J. Gregory, *Adv. Colloid Interface Sci*, 100 (2003) 475-502.
49. X.H. Zhao, Y.Q. Zhao, P. Kearney, *Environ. Technol.* 34 (2013) 263-268.
50. E. Moore, New York: *Nova Science Publishers, Inc.*, (2016) 1-92.

© 2018 The Authors. Published by ESG (www.electrochemsci.org). This article is an open access article distributed under the terms and conditions of the Creative Commons Attribution license (<http://creativecommons.org/licenses/by/4.0/>).